Conformational flexibility and role of aromatic–aromatic interactions in the crystal packing of the coordination compounds of some novel quadridentate Schiff bases

Juha T. Pulkkinen,*[a] Reino Laatikainen,[a] Markku J. Ahlgrén,[b] Mikael Peräkylä[a] and Jouko J. Vepsäläinen[a]

[a] *Department of Chemistry, University of Kuopio, PO Box 1627, FIN-70211 Kuopio, Finland*
[b] *Department of Chemistry, University of Joensuu, PO Box 111, FIN-80101 Joensuu, Finland*

Received (in Cambridge, UK) 8th October 1999, Accepted 24th December 1999
Published on the Web 29th February 2000

The synthesis and characterisation of two novel quadridentate Schiff base ligands *N*,*N*′-ethylenebis(1,5-diphenyl-4-iminopentan-2-one) (**2a**) and *N*,*N*′-ethylenebis[1,5-di(1-naphthyl)-4-iminopentan-2-one] (**2b**) and five of their Ni(II)-, Co(II)- and Cu(II) complexes are described. The crystal structures of **2a** and complexes **3**–**7** were established by single-crystal X-ray diffraction. Although the coordination geometries of **3**–**7** were found to be similar, the conformations of the aromatic side chains differed dramatically: very small changes in the coordination geometries, together with the high flexibility of the ligands, as confirmed by quantum mechanical *ab initio* calculations, seem to lead to remarkable conformational differences as well as to differences in the intermolecular aromatic–aromatic interactions and packing in the crystals.

Introduction

Fundamental organisation processes such as crystal formation, protein folding or substrate recognition by a receptor are governed by the competition between intramolecular steric energies and attractive non-covalent intermolecular forces. In the case of crystallisation, the latter are usually superficially called "packing effects" or "crystal forces" and left without further characterisation. However, the question of how much steric energy the crystal forces can compensate is relevant for the rationalisation of the crystallisation process and the crystal structure.

Flexible molecules commonly exhibit conformational isomerism which often leads to polymorphism.[1] For such compounds, molecular packing is a process in which a small alteration, for example in the crystallisation conditions, may induce a flux of strengthening events leading the system randomly to end up in any of the low wells in the flat potential surfaces. That may give rise to unpredictable conformations and molecular packing. In this work, we present an example where small differences in the coordination geometries of some isomorphic coordination compounds with flexible peripheral parts lead to unexpectedly dissimilar molecular packings. It is noteworthy that these phenomena seem to have characteristics which are analogous to the butterfly effect, a concept used by scientists studying chaotic systems.

Our original aim was to produce a molecular assembly with a reaction centre surrounded by parts of maximum flexibility capable of aromatic–aromatic interactions.[2] For the skeleton of the model we chose the quadridentate Schiff base resulting from the condensation of two equivalents of dicarbonyl compound with one equivalent of diamine. The ONNO donor atom sequence of the compounds is known to bind most metals, which makes them versatile ligands for redox active catalysts,[3] as well as for supramolecular systems.[4] The structurally simplest compound, *N*,*N*′-ethylenebis(4-iminopentan-2-one) [en(acacH)$_2$],[5] forms square planar complexes with transition metals such as Co(II), Ni(II), Cu(II), Pd(II) and Pt(II).[6] Although only the crystal structures of Cu(II)–en(acac)$_2$ are found in the literature,[7] all the square planar M(II)–en(acac)$_2$ complexes can be assumed to possess practically similar coordination geometries in the solid state, which is supported by the crystal structures of the coordination compounds of other quadridentate Schiff bases.[8]

We have recently reported a general route to 1,5-diarylpentane-2,4-diones (**1**),[9] which can be used as precursors of *N*,*N*′-ethylenebis(1,5-diaryl-4-iminopentan-2-one) (**2**), a new group of quadridentate Schiff base ligands with aromatic side chains. According to our recent study, the precursor diketones have relatively flexible structure and span a large conformational space.[10] This suggests that the C–C bonds of the aromatic side chains of their Schiff base derivatives should also have low rotational barriers and, hence, be able to adopt practically any orientation in the solid-state structure. This in fact proved to be the case when the crystal structures of their complexes **3**–**7** were examined. Moreover, the nature of the intermolecular aromatic–aromatic interactions and the molecular packings of the complexes were found to be dissimilar.

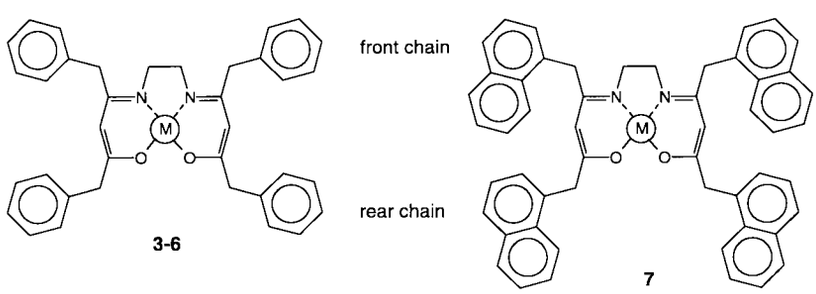

DOI: 10.1039/a908101a

In this article we present the synthesis and characterisation of two ligands and four transition metal complexes with Co(II), Ni(II) and Cu(II). Crystal structures and *ab initio* quantum mechanical calculations are used to confirm the high flexibility of the aromatic side chains of the complexes, permitting the unexpectedly divergent conformations and packings of the complexes which can be accounted for by the phenomena mentioned above. Moreover, each complex exhibits several aromatic–aromatic contacts, offering an opportunity to inspect the preference of the different types of these important interactions[2] in the solid state.

Results and discussion

Syntheses and NMR analyses

The quadridentate Schiff bases are usually easily achieved by refluxing two equivalents of a 1,3-dicarbonyl compound with one equivalent of a diamine in an alcohol. However, in some cases weak acid catalysis and/or removal of the water formed during the reaction is necessary to get appropriate yields. Since in our case both activators enhanced the reaction, we ended up with a procedure where the diketones **1** were refluxed with ethylenediamine in a Dean–Stark apparatus in the presence of a catalytic amount of *p*-TsOH in toluene leading to the ligands **2** in high yields (Scheme 1). The ^{1}H and ^{13}C NMR spectra show

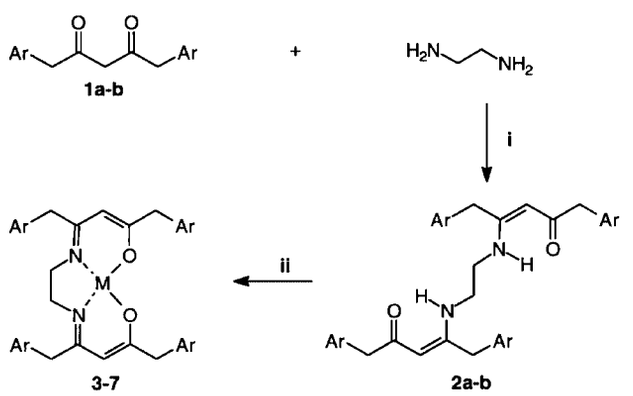

Scheme 1 Synthesis of the ligands **2** and their transition metal complexes **3**–**7**. Ar = Ph for **2a** and **3**–**6**, 1-Naph for **2b** and **7**. M = Ni^{2+} for **3**, **6** and **7**; Co^{2+} for **4**; Cu^{2+} for **5**.

typical signals for an acacenH moiety.[11] In the proton spectrum a broad NH signal is seen at 10.82–10.99 ppm. The signal is a triplet due to coupling to the protons of the ethylene bridge. Another characteristic signal for en(acacH)$_2$ type compounds is the fork-shaped multiplet of the ethylene bridge protons which in the case of **2** appears at 3.07–3.10 ppm. The carbon spectrum shows the carbonyl signal at 195.9–196.1 ppm indicating a slight delocalisation of the C–O carbon. Moreover, the compounds exist in chloroform practically solely in the ketoenamine form; the other two possible tautomers are not present in the spectra.

The complexes **3**, **5** and **7** were synthesized in quantitative yields by refluxing the corresponding ligands with Ni(II) or Cu(II) acetate in ethanol or ethanol–dichloromethane (complex **7**). We prepared also the Co(II) complex **4** but, unlike the former examples of Co(II)–en(acac)$_2$ type complexes, it was found to be unstable in solution when exposed to air. However, during the reflux the complex partly crystallised on the walls of the flask and the dry solid was found to be stable and suitable for the structure determinations. The NMR spectra were only recorded for the diamagnetic Ni complexes **3** and **7**. As expected,[12] in the ^{1}H spectrum the absence of the amino protons leads the signal of the ethylene bridge protons to collapse to a singlet and coordination shifts the signal upfield by *ca.* 0.4 ppm (2.72 ppm for **3**, 2.69 ppm for **7**). In the ^{13}C NMR spectrum, in comparison with the free ligand, the C–O signal is clearly at higher field (179.0 ppm for **3**, 179.1 ppm for **7**) indicating the carbonyl carbon to have more enolic character.

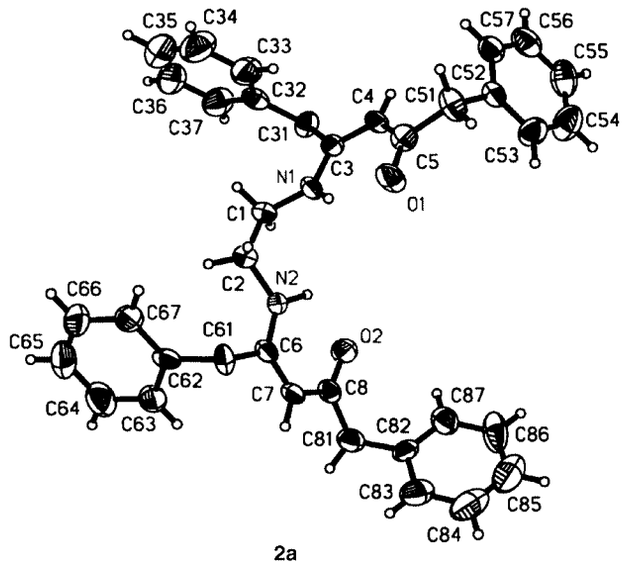

Fig. 1 Structure of the ligand **2a** showing the atom numbering scheme.

Crystal structure of the ligand

The molecular structure and atomic numbering of compound **2a** are shown in Fig. 1. The present study shows that the ligand adopts a ketoenamine structure in the solid state in agreement with former examples of en(acacH)$_2$ type ligands.[8d,13] With two exceptions,[8d,13e] the N1–C1–C2–N2 fragment has been found to adopt the *gauche* conformation. This is the case also for **2a**, the corresponding dihedral angle being −77.8°. Despite the symmetric atomic order of the ligand, the whole molecule forms an asymmetric unit belonging to the space group $P\bar{1}$, which indicates the high flexibility of the compound. Both skeletal π systems are planar, locked by an internal hydrogen bond [N1 · · · O1 = 2.672(6), N2 · · · O2 = 2.700(6) Å] and the bond lengths clearly indicate delocalisation. The carbonyl bonds [C5–O1 = 1.245(6), C8–O2 = 1.264(6) Å] are significantly longer than the average carbonyl bond length [1.23(1) Å] and, in proportion, the imine bond lengths [C3–N1 = 1.355(6), C6–N2 = 1.341(6) Å] are close to the values of the C–N bond lengths in heteroaromatics such as pyridine [1.352(5) Å].[14] In addition, the C–C bond lengths of the conjugated ketoenamine rings correspond to aromatic bond lengths. The orientations of the side chains are similar to those found in the crystal structure of the precursor diketone **1a**.[15]

Crystal structures of the complexes

Coordination geometry. The solid state structures of the metal complexes are depicted in Figs. 2 and 3, which reveal the random orientation of their side chains. The complexes **3**–**5** with the same ligand **2a** were all crystallised from ethanol and they only differ in the electronic configuration of the cation, but still large differences can be seen in their solid-state structures. A useful parameter for description of the tetrahedral distortion of the planar coordination is the angle α between the planes formed by N1–M–O1 and N2–M–O2, varying from 0 (square planar geometry) to 90° (tetrahedral geometry). Table 1 shows that the coordination geometries in this case vary from the planar Ni complex **3** [$\alpha = 2.1(3)°$] to the slightly distorted Cu complex **5** [$\alpha = 14.7(2)°$] and that the tetrahedral distortion has a significant positive correlation with the M–O and M–N bond lengths. In other words, the Ni^{2+} cation fits perfectly to the coordination ring, whereas the slightly larger Cu^{2+} forces the ligand to adopt a somewhat distorted conformation. The Co

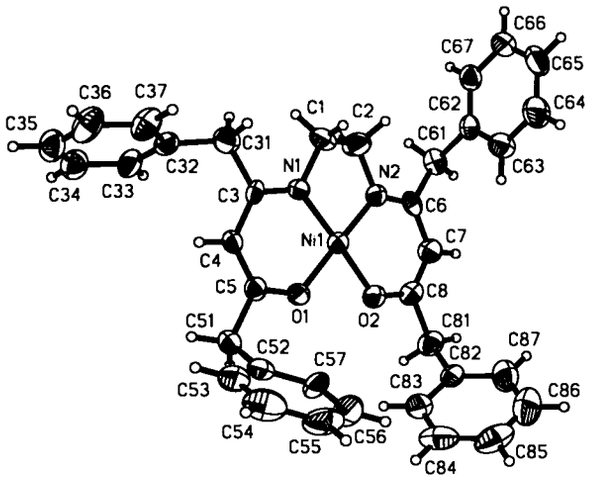

3

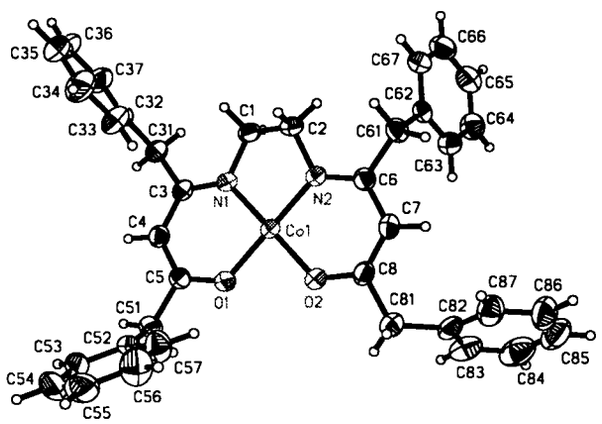

4

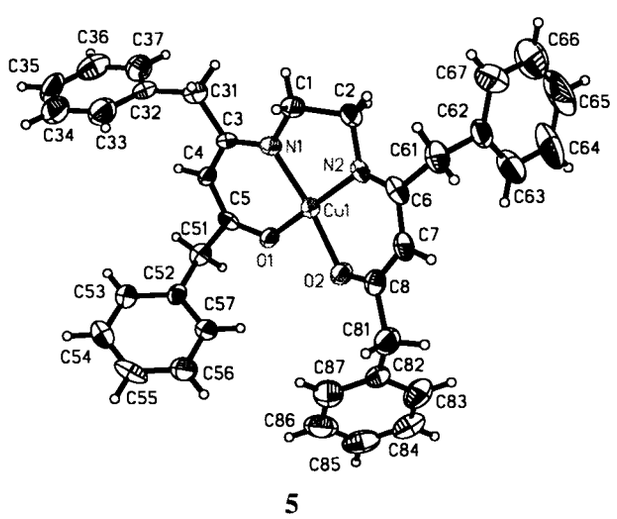

5

Fig. 2 Structures of the complexes **3**–**5** showing the atom numbering schemes.

complex **4**, the M–O and M–N bonds of which are slightly longer than in **3** but clearly shorter than in **5**, has α of 5.0(1)°. Some other parameters outlining the degree of the tetrahedral distortion are the diagonal O1–M–N2 angle (β_1) and O2–M–N1 angle (β_2) which in the case of perfect planarity have values of 180°. Table 1 reveals that β_1 and β_2 of **5** [171.7(2), 167.3(2)°] differ notably more from the plane than those of the other complexes. The correlation of the coordination bond lengths with the coordination geometry agrees with the assumption that the small differences in the tetrahedral distortion are

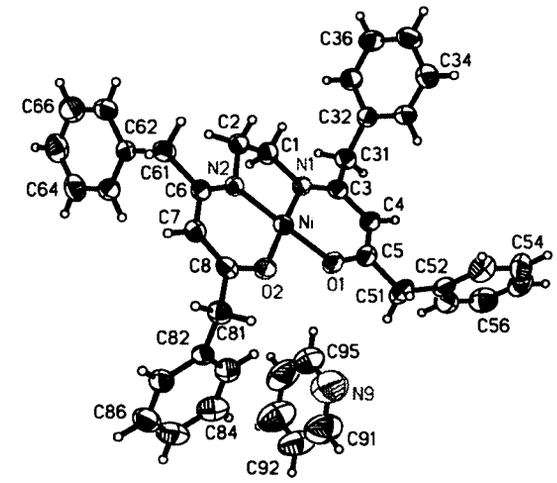

6

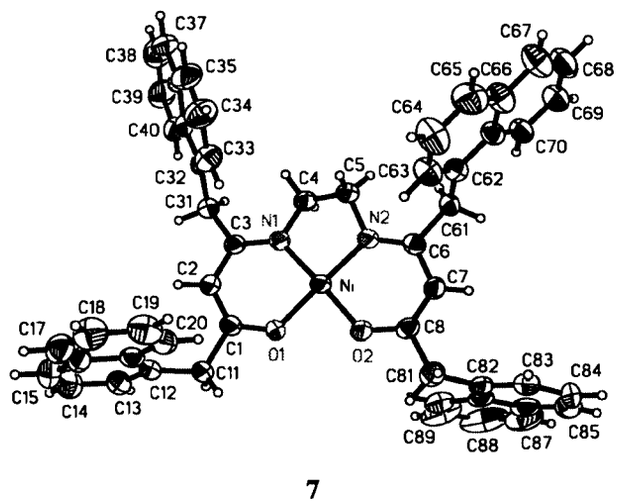

7

Fig. 3 Structures of the complexes **6** and **7** showing the atom numbering schemes.

merely caused by the metal core, not by differences in the intermolecular interactions. The previous literature reveals that in comparison to Ni(II) and Co(II) analogues, Cu(II) complexes of similar ligands always exhibit more distorted geometry.[7,8]

The Ni complex **3** was crystallised also from pyridine to see if the solvent would coordinate to the metal centre by forming an octahedral dipyridine complex. Instead, the complex **6** was found to include only one non-coordinated solvent molecule per asymmetric unit. In comparison to **3**, there is a small distortion in the coordination ring of **6** [$\alpha = 4.2(1)°$], probably due to the difference in non-covalent interaction energies caused by the pyridine. In fact, the difference between the plane angles α of **3** and **6** ($\alpha_6 - \alpha_3 = 2.1°$) makes a useful estimate for a possible distortion effect caused by a different crystal environment. Also the Ni complex **7** with the 1-naphthyl ligand **2b** was crystallised from pyridine but this complex did not include the solvent in the crystal lattice. The coordination geometry of **7** [$\alpha = 1.1(3)°$] was found similar to **3** within 1°.

Orientation of the side chains. Although the differences of the coordination sphere conformations of the complexes are small, the side chain conformations differ markedly from each other. Each complex has two pairs of identical aromatic side chains: the "front chains" are connected to the imino carbons C3 and C6, and the "rear chains" to the carbonyl carbons C4 and C7. There is a clear difference in the rotational freedom of the front and the rear chains, which is indicated by the distribution of the dihedral angles φ_i (Table 2). The rear chain rotations about the

Table 1 The angles between the planes defined by O1–M–N1 and O2–M–N2 (a/°), the M–O and M–N bond lengths (Å), and the diagonal angles (O1–M–N2, O2–M–N1, β/°) of the complexes

	3	**4**	**5**	**6**	**7**
a	2.1(3)	5.0(1)	14.7(2)	4.2(1)	1.1(3)
M–O1	1.842(3)	1.852(1)	1.899(3)	1.836(2)	1.846(2)
M–O2	1.845(3)	1.854(1)	1.939(3)	1.847(1)	1.849(2)
M–N1	1.854(4)	1.862(1)	1.945(4)	1.862(2)	1.858(3)
M–N2	1.851(4)	1.858(1)	1.938(4)	1.846(2)	1.861(3)
β_1 (O1–M–N2)	176.5(2)	176.1(1)	171.7(2)	175.6(1)	178.2(1)
$180° - \beta_1$	3.5	3.9	8.3	4.4	1.8
β_2 (O2–M–N1)	177.4(2)	175.9(1)	167.3(2)	176.4(1)	177.9(1)
$180° - \beta_2$	2.6	4.1	12.7	3.6	2.1

Table 2 The side chain dihedral angles (°) of the complexes **3**–**7**

	3	**4**	**5**	**6**	**7**
φ_1, C4–C5–C51–C52	−103.5(5)	105.1(2)	−103.4(5)	7.8(4)	30.2(5)
φ_2, C7–C8–C81–C82	121.1(5)	33.5(3)	−153.5(5)	105.9(2)	39.9(5)
φ_3, C4–C3–C31–C32	−19.0(7)	−95.4(2)	5.9(7)	−95.9(2)	−111.7(3)
φ_4, C7–C6–C61–C62	−108.3(5)	−96.1(2)	103.0(5)	−100.4(2)	98.2(3)
θ_1, C5–C51–C52–C53	114.7(4)	−135.8(2)	111.5(4)	92.6(3)	−114.2(4)
θ_2, C8–C81–C82–C83	83.7(5)	98.0(2)	101.4(4)	55.7(3)	−110.7(4)
θ_3, C3–C31–C32–C33	−60.1(5)	2.5(3)	82.5(5)	50.8(3)	12.4(5)
θ_4, C6–C61–C62–C63	36.2(5)	50.3(2)	−54.7(6)	32.8(3)	5.2(5)

C5–C51 and C8–C81 bonds are expected to have a relatively low twofold barrier, the height of which is mainly governed by steric and electrostatic repulsions between the phenyl rings and the C=O or the C–H groups (for the *ab initio* quantum mechanical calculations, see below). Of the ten φ_1 and φ_2 values, four have practically the same magnitude ($|\varphi| = 103.4$–$105.9°$), which can be assumed to correspond to the potential energy minima. However, the high rotational freedom of the rear chains allows the side chains to reflect the small differences in the coordination geometry, which is indicated by the wide distribution of the remaining six dihedral angle values. On the other hand, eight of the ten φ_3 and φ_4 values ($|\varphi| = 95.4$–$111.7°$) show that, due to the steric hindrance caused by the bulky ethylene group connected to the imino nitrogen, the front chain rotations are notably restricted. Nevertheless, there are some variations in the values ($\Delta|\varphi|_{max} = 16.3°$) which might partly be due to differences in the planarity of the complexes. The computational results concerning the chain rotations are discussed below.

The conformational behaviour of the aryl rings for benzyl derivatives is described by a potential function having a twofold rotational barrier.[16] For the precursor diketone **1a**, the most stable conformation is the one with the aryl π plane perpendicular to the C=O bond ($\theta_i = 90°$), the rotational barrier, however, being relatively small.[10,15] This high degree of freedom is manifested by the wide distribution of the aryl dihedral angles θ_i shown in Table 2. Again, especially for the front chain aryl rings, the notably divergent θ_i values can be interpreted as consequences of the small differences between the coordination geometries of the complexes.

Crystal packing and aromatic–aromatic interactions. The previous studies on the aromatic–aromatic interactions strongly suggest that a benzene dimer favours T-shaped orientations in any state of matter,[2] whereas face-to-face (FF) stacking is usually exhibited by aromatic moieties having opposite partial charges (C_6H_6–C_6F_6, for example)[2c] or by ring systems larger than a phenyl group.[2a] According to the theoretical calculations by Jorgensen and Severance,[2a] the global minimum for the benzene dimer is the edge-to-face (EF) structure with the ring centre–ring centre (c–c) separation of 5.0 Å, while the point-to-face (PF) and "parallel-displaced" FF orientations with 5.2 and 4.5 Å c–c distances, respectively, had *ca.* 0.7–0.8 kJ mol^{-1} higher interaction energies.

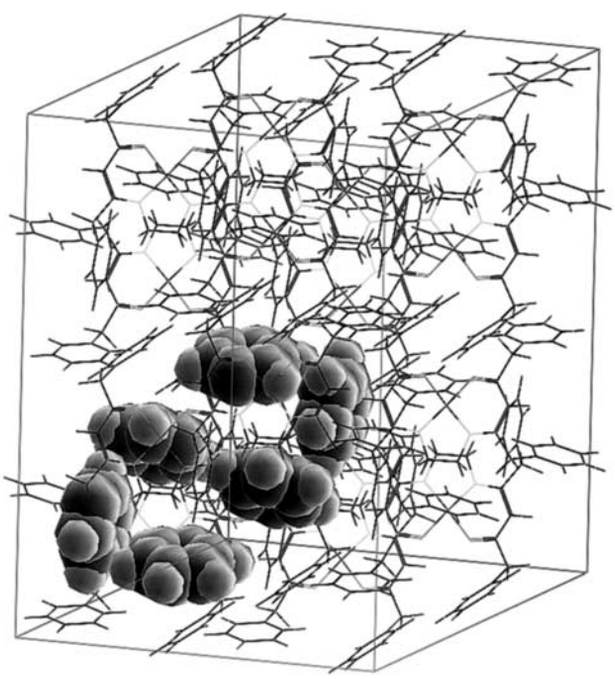

Fig. 4 Molecular packing and aromatic–aromatic interactions of complex **3**. The four EF contacts present within a centrosymmetric pair are highlighted with the space-filled phenyl rings.

The solid-state aromatic–aromatic interactions of the complexes **3**–**7** were found to prefer the T-shaped orientations, although "parallel displaced" FF stacking was present in three examples. The Figs. 4–8 visualise the differences in the molecular packings of the complexes **3**–**7** as well as the different types of aromatic–aromatic interactions between the side chains. The crystal lattice of the Ni complex **3** (see Fig. 4) consists of centrosymmetric pairs (the shortest interatomic distance N1 ··· C3 = 4.0 Å) interacting with four mutual EF contacts. First, the phenyl groups C(62–67) form an EF interaction with the C(52–57) rings having c–c distances of 5.2 Å and plane angles of 88° between the aromatic rings. However, the C(52–57) "edges" are shifted by 1.4 Å from the centres of the "faces", due to which the ring–ring orientations are L- rather than T-shaped. Also the contacts between the C(32–37)

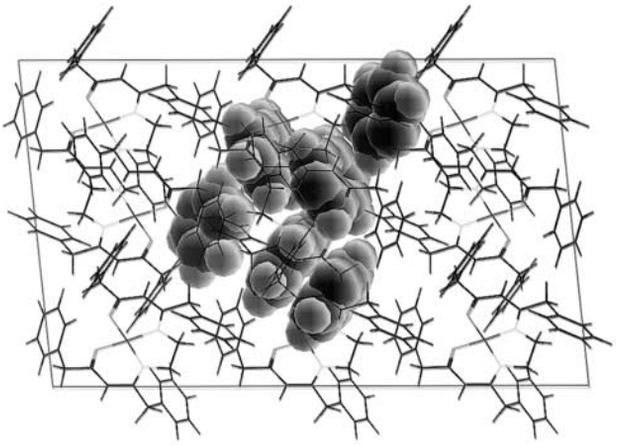

Fig. 5 Molecular packing and aromatic–aromatic interactions of complex **4** viewed along the crystallographic *c* axis. The three EF and two FF contacts form the aromatic–aromatic network.

and C(62–67) rings are incomplete EF interactions with c–c distances of 5.3 Å, plane angles of 88° and 1.5 Å shifts of the "edges". Nevertheless, in the case of **3** the aromatic–aromatic interactions undoubtedly contribute significantly to the packing of the crystals by stabilising the molecular network, although none of them was found to act between the centrosymmetric pairs.

A completely opposite trend was found for the Co complex **4** (see Fig. 5): there were no aromatic–aromatic interactions present within the centrosymmetric dimers (N1 · · · N1 distance of 3.6 Å) but, instead, a network of two FF stackings and three EF contacts between the pairs was found. The "parallel displaced" FF interactions are formed between all the C(32–37)–C(32–37) and C(82–87)–C(82–87) ring pairs with interplanar separation distances of 3.5 Å and c–c distances of 4.5 and 4.7 Å, respectively. In addition, the rings C(32–37) and C(52–57) form two types of EF contacts with one exhibiting precisely the central position (c–c = 5.1 Å, plane angle = 70°) and the other having a shift of 0.8 Å (c–c = 5.2 Å, plane angle = 70°). The third EF interaction between C(32–37) and C(82–87) is the most incomplete one in **4** (c–c = 5.6 Å, plane angle = 63°, shift = 0.6 Å) but, nevertheless, clearly is a part of the aromatic–aromatic network spread throughout the crystal. As the only structural difference between **3** and **4** is the coordinated metal introducing a negligible distortion of 2.1 and 5.0°, respectively, the total unlikeness of the molecular packing and the organisation of aromatic–aromatic contacts is an unexpected result and definitely related to the distortion.

Also the complex **5** forms dimers (Cu · · · C7 distance of 3.2 Å) along the *c* axis of the crystal lattice but unlike **3** or **4** the molecule pair is not centrosymmetric. Nevertheless, the dimers exhibit a global construction of aromatic–aromatic contacts interacting both within and between the dimers (see Fig. 6). The C(32–37) and C(52–57) phenyl rings of **5** form a network of two PF and one EF interaction with respect to which the PF contact C(32–37)–C(52–57), present within a dimer, has an exactly perpendicular arrangement (plane angle 90°) with the "point" directed precisely to the centre of the "face" with a c–c separation of 5.4 Å. Also the EF interactions, which are found between the molecule pairs, exhibit a perpendicular arrangement but the position of the rings is of the L type with a 1.8 Å deviation from the optimum site. The PF contact between two C(32–37) rings has a plane angle of 67° and the "point" is slightly (0.4 Å) shifted from the optimum position and c–c distance (5.5 Å). In addition to the T interaction network, there is also one intermolecular aromatic stacking interaction per molecule present in the crystal structure of **5**. The parallel displaced FF orientation is formed by two C(62–67) rings, with an interplanar separation of 3.7 Å and c–c distance of 4.8 Å. Altogether, the aromatic–aromatic interactions of **5** form a

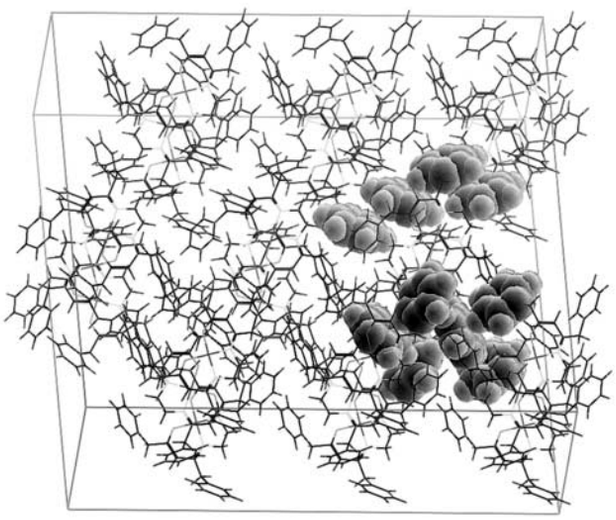

Fig. 6 Molecular packing and aromatic–aromatic interactions of complex **5** which form separate chains of π–π stacking (upper) and T-shaped (lower) interactions.

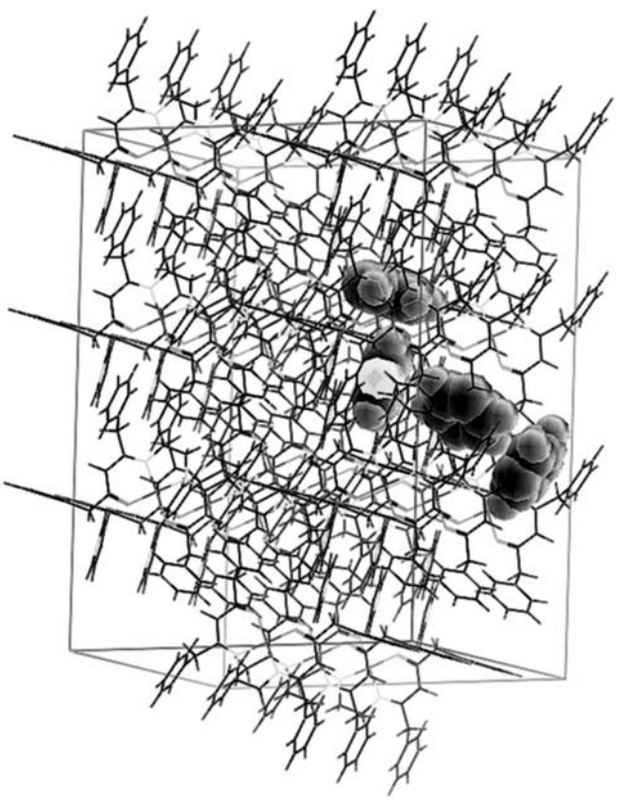

Fig. 7 Molecular packing and aromatic–aromatic interactions of complex **6**. The aromatic–aromatic network is formed by the solvent pyridine (second highlighted ring from the left) and three phenyl rings all connected to different molecular units.

uniform network in which three out of the four aromatic rings participate. As the tetrahedral distortion of **5**, induced by the metal core, is clearly stronger than those of **3** and **4** it undoubtedly furthers the complicated appearance of the ring–ring interactions.

In the crystal structure of the complex **6** the pyridine solvent and the three side chain phenyl groups, all bound to a different molecular unit, form constructions of three EF interactions throughout the crystal lattice (see Fig. 7). The solvent molecule is clathrated with two separate EF contacts in which it acts as an "edge" for C(52–57) (c–c 5.1 Å, displacement 1.2 Å, plane angle 89°) and as a "face" for C(82–87) (c–c 5.4 Å, displacement 0.3 Å, plane angle 81°). The third EF contact

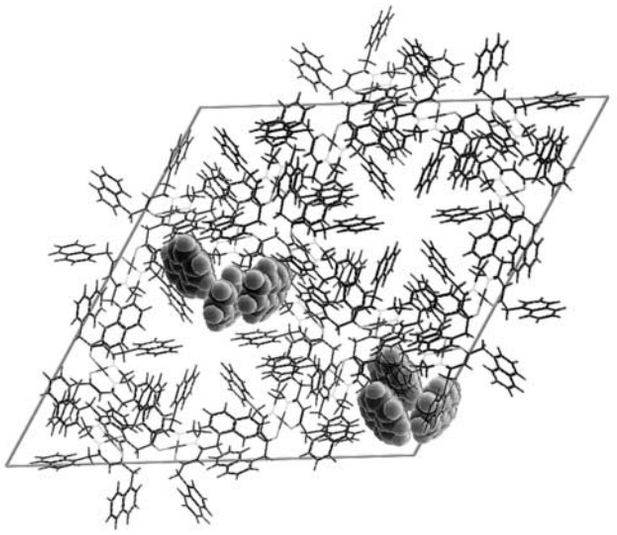

Fig. 8 Molecular packing and aromatic–aromatic interactions of complex **7** viewed along the crystallographic *c* axis. The figure reveals the "hexagonal wheels" which are packed to form channels stabilised by EF and FF interactions.

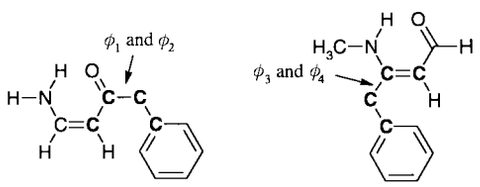

Fig. 9 Quantum mechanical model systems used to calculate the barriers of the rear (φ_1 and φ_2) and the front (φ_3 and φ_4) chain rotations.

is formed between C(82–87) and C(62–67) (c–c 5.0 Å, displacement 1.4 Å, plane angle 80°). Since the only difference between **3** and **6** is the presence of the solvent in the crystal lattice, the dissymmetric side chain orientations, aromatic–aromatic interactions and organisation of the crystal lattice can be accounted for by differences in the non-covalent interaction energies. The molecular units form centrosymmetric pairs also in the case of **6** (N1 · · · N1 distance of 3.7 Å).

In comparison to the other complexes, the molecular packing of the naphthyl analogue **7** is totally different as indicated by the space group ($R\bar{3}$). The centrosymmetric pairs (C6 · · · C6 distance of 4.5 Å) have organised in such a way that the C(32–41) rings are directed at the same point forming a wheel-like arrangement with a hexagonal hole in the middle. The "wheels" are packed in layers forming hexagonal channels along the crystallographic *c* axis (see Fig. 8) and, as expected, aromatic–aromatic interactions are involved in the crystal formation. As previously shown,[2a] aromatic moieties larger than benzene have a clear tendency to favour face-to-face stacking interactions in the solid state. However, complex **7** exhibits two individual aromatic–aromatic contacts per molecular unit both formed between the C(32–41) and C(82–91) rings, constructing an infinite network of alternating FF (parallel displaced, interplanar distance 3.7 Å, c–c 4.7 Å) and EF (c–c 5.0 Å) pairs.

Computational studies

Ab initio quantum mechanical calculations (GAUSSIAN94 program[17]) were carried out to study the flexibility of the aromatic side chains by calculating energy profiles for the rotation of the side chain dihedral angles φ_1 (φ_2) and φ_3 (φ_4) using reduced models of the complexes **3**–**6** (see Fig. 9). The energy profiles were calculated by rotating the dihedral angles in steps of 45°, optimising the geometry in every point at the HF/6-31+G* level and calculating the energy at the MP2/6-31+G* level using the optimised geometry (MP2/6-31+G*//HF/6-31+G*). In every step only the dihedral angle was kept frozen and all the other geometric parameters were allowed to optimise freely. In addition, full geometry optimisations were done in order to locate the minimum structures. The energies reported are calculated at the MP2/6-31+G*//HF/6-31+G* level. The torsion profiles calculated using the model systems are thought to reproduce at least qualitatively the corresponding profiles of the whole complexes. The energy profile for the rotations of φ_1 and φ_2 (the rear chain rotations) is shown in Fig. 10 and the profile of φ_3 and φ_4 (the front chain rotations) in Fig. 11. The values of the corresponding dihedral angles of the crystal structures are marked in the figures with triangles.

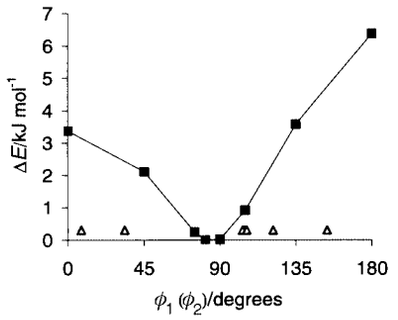

Fig. 10 Energy profile for the rear chain rotations φ_1 and φ_2 calculated at the MP2/6-31+6*//HF/6-31+G* level. The values of the corresponding angles of the solid-state structures of complexes **3**–**6** are shown with triangles.

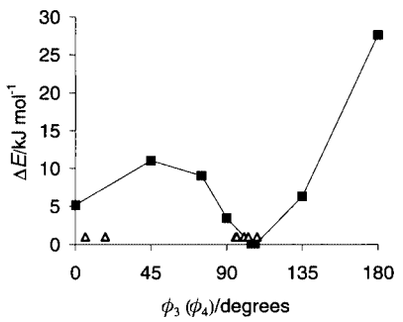

Fig. 11 Energy profile for the front chain rotations φ_3 and φ_4. Details as in Fig. 10.

The energy barriers calculated for the rear chain rotations are 3.4 (located at 0) and 6.4 kJ mol^{-1} (at 180°). The barriers are small and indicate that φ_1 and φ_2 can rotate almost freely in the complexes **3**–**7**. This agrees with the wide distribution of the torsion angles of the crystal structures. In the energy profile of the front chain rotations there are two minima located at 107 and 0°. The minimum at 0° is calculated to be 5.2 kJ mol^{-1} higher in energy than the global minimum. The two minima are separated by energy barriers of 11.0 (located at 45) and 27.6 kJ mol^{-1} (at 180°). The two barriers restrict the rotation of torsion angles φ_3 and φ_4 of the aromatic side chain considerably. The shape of the calculated rotation barrier is nicely reflected in the distribution of the torsion angles φ_3 and φ_4 observed in the crystal structures: six out of eight torsion angles are close to the calculated global minimum and the remaining two are close to the local minimum at 0°. In general, the calculated results are in good agreement with the experiments and support the conclusions drawn from the X-ray data about the flexibility of the side chains.

Conclusions

The results presented above confirm the high flexibility of the peripheral groups in the compounds. Although the differences in the coordination geometries of the complexes **3**–**7** are small, the side chain conformations, especially in the case of the rear

Table 3 Crystallographic data for the ligand **2a** and the complexes **3**–**7**

	2a	**3**	**4**	**5**	**6**	**7**
Formula	$C_{36}H_{36}N_2O_2$	$C_{36}H_{34}N_2NiO_2$	$C_{36}H_{34}CoN_2O_2$	$C_{36}H_{34}CuN_2O_2$	$C_{36}H_{34}N_2NiO_2{\cdot}C_5H_5N$	$C_{52}H_{42}N_2NiO_2$
M	528.67	585.36	585.58	590.19	664.46	785.59
Crystal system	Triclinic	Triclinic	Triclinic	Monoclinic	Triclinic	Trigonal
Space group	$P\bar{1}$	$P\bar{1}$	$P\bar{1}$	$P2_1/c$	$P\bar{1}$	$R\bar{3}$
a/Å	10.067(2)	10.035(3)	9.811(1)	25.850(5)	10.1650(10)	40.3445(8)
b/Å	10.796(2)	12.473(3)	11.872(4)	13.195(3)	11.118(2)	40.3445(8)
c/Å	13.606(3)	12.724(4)	12.858(2)	8.711(2)	15.414(2)	13.9251(8)
α/°	97.28(3)	69.94(3)	86.73(2)	90	75.32(2)	90
β/°	96.24(3)	81.79(3)	81.97(1)	93.26(3)	88.28(2)	90
γ/°	97.08(3)	83.42(3)	83.69(2)	90	88.59(2)	120
V/Å^3	1444.0(5)	1477.0(7)	1472.7(6)	2966.4(11)	1684.1(4)	19629.0(13)
T/K	293(2)	293(2)	293(2)	293(2)	293(2)	293(2)
Z	2	2	2	4	4	18
μ/mm^{-1}	0.075	0.692	0.618	0.771	0.616	0.486
Measured reflections	4361	4390	7195	5587	11465	15314
Unique reflections	4256	4390	6799	5233	6746	7660
R [$I > 2\sigma(I)$]	0.074	0.077	0.035	0.049	0.030	0.062
wR (F^2, all data)	0.105	0.087	0.085	0.073	0.059	0.112

chains, are widely distributed. Of the ten φ_1 and φ_2 values, only four are close to the calculated global minimum while the remaining six are randomly distributed to the potential energy surface. The same is true for the ten θ_3 and θ_4 angles: only one value is close to 90°, which corresponds to the minimum energy conformation.

The randomness is true also for the molecular packing of the complexes which varies unpredictably, manifested in different combinations of face-to-face, edge-to-face and point-to-face aromatic–aromatic interactions. In all the examples presented above, aromatic–aromatic interactions have a major role in the construction of the molecular assemblies in the solid state. Altogether, there are nine EF, three FF and two PF contacts present in the crystal lattices of complexes **3**–**6**, a distribution which agrees nicely with the previous theoretical results that the EF interaction clearly is the energetically most favoured form for phenyl rings. In addition, the results reflect the broadness of the potential well related to aromatic–aromatic interactions as indicated by the small energy differences between the interaction types,[2a] or more generally, the fact that, as a function of distance, attractive van der Waals forces decay rather slowly.

On the grounds of the present results it is impossible to decide whether the small differences in the coordination geometry really are, even partly, the cause of the dissimilar packing of the complexes, since the tendency of the complexes to exhibit polymorphism under a variety of crystallisation conditions is not known. Nevertheless, whatever the explanation, the crystallisation process of the isomorphic flexible compounds presented here is unpredictable, where a negligible difference in the prevailing circumstances, such as molecular geometry or crystallisation conditions, can lead to unexpected dissimilarity of the conformations and packing of the molecular units. Such a process clearly is analogous to the butterfly effect.

Experimental

General

All chemicals and solvents were reagent grade and used as received. The precursor diketones were prepared according to our previous general procedure.[9] Melting points were measured with a Stuart Scientific SMP2 apparatus and are uncorrected. ^{1}H and ^{13}C NMR spectra (TMS/$CDCl_3$) were recorded on a Bruker AM 400 WB spectrometer operating at 400 and 101 MHz, respectively. All the coupling constants are given in Hz. Mass spectra were obtained on a Varian VG 70-250SE spectrometer. Elemental analyses were performed with a Carlo Erba 1106 elemental analyzer.

Details of crystal parameters and structure determinations of compounds **2a** and **3**–**7** are summarised in Table 3. Non-hydrogen atoms were refined anisotropically but the aromatic 6-membered rings as rigid groups in **3** and **4**. The hydrogen atoms were placed at calculated positions and not refined except for the OH hydrogen atoms in **2a** which were located from difference Fourier maps and refined with a fixed isotropic thermal parameter (U_{iso} = 0.08 Å^2).

CCDC reference number 188/217. See http://www.rsc.org/suppdata/p2/a9/a908101a/ for crystallographic files in .cif format.

General procedure for the synthesis of the free ligands 2

A solution of the diketone **1** (2 mmol), ethylenediamine **2** (1 mmol) and *p*-TsOH (0.1 mmol) in toluene (8 ml) was refluxed in a Dean–Stark apparatus for 16 h. After cooling to room temperature, the solution was dried *in vacuo*, the residue dissolved in CH_2Cl_2 and washed with water. The organic phase was dried *in vacuo* giving a brown viscous oil to which 50 : 50 ethyl acetate–*n*-hexane was added. The solid product, which separated as a white powder, was filtered off and evaporated to dryness. Compound **2a** was recrystallised from chloroform.

***N*,*N*′-Ethylenebis(1,5-diphenyl-4-iminopentan-2-one) (2a).** Yield 91%; mp 162.5–163.5 °C; δ_H 10.82 (2 H, br t, N*H*), 7.30–7.19 (16 H, m, H_{Ar}), 7.08–7.06 (4 H, m, H_{Ar}), 4.96 (2 H, s, C*H*), 3.55 (4 H, s, CH_2), 3.35 (4 H, s, CH_2), 3.07 (4 H, m, CH_2); δ_C 195.9, 164.6, 137.1, 135.7 (4 s), 129.3, 128.8, 128.4, 128.4, 127.0, 126.3, 96.5 (7 d), 49.1, 43.4, 38.3 (3 t); *m*/*z* (Found: M$^+$, 528.27575. $C_{36}H_{36}N_2O_2$ requires 528.27768) 528 (M$^+$, 1%), 437 (58), 319 (45), 278 (38), 264 (33), 186 (97), 173 (52), 91 (100).

***N*,*N*′-Ethylenebis[1,5-di(1-naphthyl)-4-iminopentan-2-one] (2b).** Yield 87%; mp 184.5–185.5 °C; δ_H 10.99 (2 H, br t, *J* 6.1, N*H*), 7.93 (2 H, d, *J* 8.4, H_{Ar}), 7.79 (2 H, d, *J* 7.1, H_{Ar}), 7.77 (2 H, d, *J* 7.1, H_{Ar}), 7.68 (2 H, d, *J* 8.1, H_{Ar}), 7.67 (2 H, d, *J* 8.1, H_{Ar}), 7.53 (2 H, d, *J* 8.6, H_{Ar}), 7.45–7.28 (10 H, m, H_{Ar}), 7.24 (2 H, d, *J* 7.1, H_{Ar}), 7.22 (2 H, dd, *J* 8.2, 7.1, H_{Ar}), 7.02 (2 H, d, *J* 7.1, H_{Ar}), 4.87 (2 H, s, C*H*), 3.93 (4 H, s, CH_2), 3.61 (4 H, s, CH_2), 3.10 (4 H, m, CH_2); δ_C 196.1, 165.1, 134.0, 133.8, 133.8, 132.6, 131.8, 131.7 (8 s), 128.9, 128.8, 128.1, 128.0, 127.5, 126.6, 126.2, 126.1, 126.1, 125.7, 125.7, 125.6, 124.7, 123.3, 96.9 (15 d), 47.0, 43.8, 35.3 (3 t); *m*/*z* (Found: M$^+$ − C_8H_6, 626.29333. $C_{44}H_{38}N_2O_2$ requires 626.26813) 626 (M$^+$ − C_8H_6, 11%), 560 (6), 419 (77), 392 (7), 210 (26), 141 (100).

General procedure for the synthesis of the complexes 3–7

The free ligand **2** (0.085 mmol) was dissolved in 6 ml of refluxing EtOH (4 ml CH_2Cl_2 for **7**). The appropriate M(AcO)$_2{\cdot}n$H$_2$O (0.085 mmol) in 3 ml of EtOH was then added and the resulting

mixture refluxed for 1 h. After cooling to room temperature, the solvent was removed *in vacuo* and the solid residue recrystallised from ethanol (**6** and **7** from pyridine).

***N*,*N*′-Ethylenebis(1,5-diphenyl-4-iminopent-2-en-2-olato)-nickel(II) (3).** Yield 94%, reddish brown needles, mp 156.5–157.0 °C (decomp.) (Found: C, 74.05; H, 5.64; N, 4.46. $C_{36}H_{34}N_2O_2Ni$ requires C, 73.87; H, 5.85; N, 4.79%); δ_H 7.32–7.15 (16 H, m, H_{Ar}), 7.04–7.01 (4 H, m, H_{Ar}), 4.81 (2 H, s, CH), 3.47 (4 H, s, CH_2), 3.42 (4 H, s, CH_2), 2.72 (4 H, s, CH_2); δ_C 179.0, 165.7, 138.1, 136.1 (4 s), 129.3, 128.7, 128.2, 128.0, 126.6, 126.1, 100.3 (7 d), 53.1, 44.6, 40.3 (3 t); *m*/*z* 585 (M^+, 100%), 529 (6), 332 (2), 316 (12), 288 (10), 277 (2).

***N*,*N*′-Ethylenebis(1,5-diphenyl-4-iminopent-2-en-2-olato)-cobalt(II) (4).** Orange red plates, mp 144.5–146.0 °C (decomp.) (Found: C, 73.48; H, 5.86; N, 4.66. $C_{36}H_{34}N_2O_2Co$ requires C, 73.84; H, 5.85; N, 4.78%).

***N*,*N*′-Ethylenebis(1,5-diphenyl-4-iminopent-2-en-2-olato)-copper(II) (5).** Yield 98%, dark violet needles; mp 128–129 °C (decomp.) (Found: C, 72.97, H, 5.80, N, 4.78. $C_{36}H_{34}N_2O_2Cu$ requires C, 73.26; H, 5.81; N, 4.75%); *m*/*z* 590 ($M + H^+$, 54%), 499 (2), 396 (6), 295 (10), 277 (100).

***N*,*N*′-Ethylenebis(1,5-diphenyl-4-iminopent-2-en-2-olato)-nickel(II) pyridine solvate (6).** Brown prisms; complex **3** was dissolved in pyridine and allowed to evaporate at ambient temperature to give crystals which included one solvent molecule per asymmetric unit.

***N*,*N*′-Ethylenebis[1,5-di(1-naphthyl)-4-iminopent-2-en-2-olato]nickel(II) (7).** Yield 95%, reddish brown prisms; mp 201.5–203.0 °C (decomp.); δ_H 7.99 (2 H, m, H_{Ar}), 7.85–7.51 (10 H, m, H_{Ar}), 7.49–7.16 (14 H, m, H_{Ar}), 7.04 (2 H, m, H_{Ar}), 4.59 (2 H, s, CH), 3.95 (4 H, s, CH_2), 3.68 (4 H, s, CH_2), 2.69 (4 H, s, CH_2); δ_C 179.1, 166.1, 134.3, 133.7, 133.5, 132.4, 131.7, 131.3 (8 s), 128.8, 128.3, 127.7, 127.3, 127.1, 126.1, 125.8, 125.7, 125.5, 125.4, 125.4, 125.0, 124.9, 122.7, 100.5 (15 d), 53.1, 42.2, 37.2 (3 t).

Acknowledgements

We thank Mr Jukka Knuutinen (Dept. Pharm. Chem., Univ. Kuopio) for performing the mass measurements, Dr Sirpa Peräniemi (Dept. Chem., Univ. Joensuu) for the elemental analyses and Mrs Maritta Salminkoski (Dept. Chem., Univ. Kuopio) for technical assistance. This work was financially supported by the Northern Savo Fund of the Finnish Cultural Foundation and the Academy of Finland.

References

1 J. Bernstein and A. T. Hagler, *J. Am. Chem. Soc.*, 1978, **100**, 673; J. Royer, C. Décoret, B. Tinland, M. Perrin and R. Perrin, *J. Phys. Chem.*, 1989, **93**, 3393; L. P. Burke, A. D. DeBellis, H. Fuhrer, H. Meier, S. D. Pastor, G. Rihs, G. Rist, R. K. Rodebaugh and S. P. Shum, *J. Am. Chem. Soc.*, 1997, **119**, 8313; T. Wagner and U. Englert, *Struct. Chem.*, 1997, **8**, 357; M. A. Buntine, V. J. Hall, F. J. Kosovel and E. R. T. Tiekink, *J. Phys. Chem. A*, 1998, **102**, 2472; S.-L. Jia, W. Jentzen, M. Shang, X.-Z. Song, J.-G. Ma, W. R. Scheidt and J. A. Shelnutt, *Inorg. Chem.*, 1998, **37**, 4402.

2 (*a*) W. L. Jorgensen and D. L. Severance, *J. Am. Chem. Soc.*, 1990, **112**, 4768 and the references therein; (*b*) C. A. Hunter and J. K. M. Saunders, *J. Am. Chem. Soc.*, 1990, **112**, 5525; (*c*) R. Laatikainen, J. Ratilainen, R. Sebastian and H. Santa, *J. Am. Chem. Soc.*, 1995, **117**, 11006 and the references therein.

3 T. Nagata, K. Yorozu, T. Yamada and T. Mukaiyama, *Angew. Chem., Int. Ed. Engl.*, 1995, **34**, 2145; J. L. Leighton and E. N. Jacobsen, *J. Org. Chem.*, 1996, **61**, 389.

4 D. M. Rudkevich, Z. Brzozka, M. Palys, H. C. Visser, W. Verboom and D. N. Reinhoudt, *Angew. Chem., Int. Ed. Engl.*, 1994, **33**, 467.

5 M. A. Combes, *C. R. Acad. Sci.*, 1889, **108**, 1252.

6 G. T. Morgan and J. D. M. Smith, *J. Chem. Soc.*, 1925, **128**, 2030; 1926, **129**, 912; P. J. McCarthy, R. J. Hovey, K. Ueno and A. E. Martell, *J. Am. Chem. Soc.*, 1955, **77**, 5820.

7 D. Hall, A. D. Rae and T. N. Waters, *J. Chem. Soc.*, 1963, 5897; D. Hall, H. J. Morgan and T. N. Waters, *J. Chem. Soc. A*, 1966, 677; G. R. Clark, D. Hall and T. N. Waters, *J. Chem. Soc. A*, 1969, 823; E. N. Baker, D. Hall and T. N. Waters, *J. Chem. Soc. A*, 1970, 396.

8 (*a*) E. Larsen, S. Larsen, S. Røen and K. J. Watson, *Acta Chem. Scand., Ser. A*, 1976, **30**, 125; (*b*) H. C. Allen, G. L. Hillhouse and D. J. Hodgson, *Inorg. Chim. Acta*, 1979, **37**, 37; (*c*) S. Z. Haider, A. Hashem, K. M. A. Malik and M. B. Hursthouse, *J. Bangladesh Acad. Sci.*, 1980, **4**, 139; (*d*) J. N. Fernández-G., R. G. Enríguez, A. Tobón-Cervantes, M. I. Bernal-Uruchurtu, R. Villena-I., W. F. Reynolds and J-. P. Yang, *Can. J. Chem.*, 1993, **71**, 358.

9 J. T. Pulkkinen and J. J. Vepsäläinen, *J. Org. Chem.*, 1996, **61**, 8604.

10 J. T. Pulkkinen, R. Laatikainen, J. J. Vepsäläinen and M. J. Ahlgrén, *Magn. Reson. Chem.*, 1999, **37**, 119.

11 G. O. Dudek and R. H. Holm, *J. Am. Chem. Soc.*, 1961, **83**, 2099.

12 P. J. McCarthy and A. E. Martell, *Inorg. Chem.*, 1967, **6**, 781.

13 (*a*) N. Bresciani-Pahor, M. Calligaris, G. Nardin, L. Randaccio and D. Viterbo, *Acta Crystallogr., Sect. B*, 1979, **35**, 2776; (*b*) N. Berth, E. Larsen and S. Larsen, *Tetrahedron*, 1981, **37**, 2477; (*c*) R. Cea-Olivares, I. Rodríguez, M. Soriano-García, R. A. Toscano and M. Córdoba, *Monatsh. Chem.*, 1984, **115**, 485; (*d*) R. Cea-Olivares, I. Rodríguez, M. J. Rosales and A. Toscano, *Aust. J. Chem.*, 1984, **37**, 879; (*e*) S. Z. Haider, A. Hashem, K. M. A. Malik and M. B. Hursthouse, *J. Bangladesh Acad. Sci.*, 1981, **5**, 85.

14 *CRC Handbook of Chemistry and Physics*, 66th edition, eds. R. C. Weast, M. J. Astle and W. H. Beyer, CRC Press, Inc., Boca Raton, FL, 1986, p. F-188.

15 J. T. Pulkkinen and M. J. Ahlgrén, *Acta Crystallogr., Sect. C*, 1999, **55**, IUC 9900142.

16 W. J. E. Parr and T. Schaefer, *Acc. Chem. Res.*, 1980, **13**, 400.

17 M. J. Frisch, G. W. Trucks, H. B. Schlegel, P. M. W. Gill, B. G. Johnson, M. A. Robb, J. R. Cheeseman, T. A. Keith, G. A. Petterson, J. A. Montgomery, K. Rachavachari, M. A. Al-Laham, V. G. Zakrzewski, J. V. Ortiz, J. B. Foresman, J. Cioslowski, B. B. Stefanov, A. Nanayakkara, M. Challacombe, C. Y. Peng, P. Y. Ayala, W. Chen, M. W. Wong, J. L. Andres, E. S. Replogle, R. Gomperts, R. L. Martin, D. J. Fox, J. S. Binkley, D. J. Defrees, J. Baker, J. J. P. Stewart, M. Head-Gordon, C. Gonzales and J. A. Pople, GAUSSIAN94, Revision E.3., Gaussian Inc., Pittsburgh, PA, 1995.

Paper a908101a